Rolling and whip phenomenon of hollow rotor slipping on internal stator

A. N. Nikiforov
Mechanical Engineering Research Institute of the Russian Academy of Sciences, Moscow, Russia
E-mail: *n.andre@mail.ru*

Received 10 December 2022; received in revised form 20 January 2023; accepted 2 February 2023
DOI https://doi.org/10.21595/mme.2023.23104

Abstract. Dynamic features of a rotor that rolls without or with whipping and slipping of own inner surface on a rigid stator are discussed. Change in the whirling direction associated with the rolling of the rotor from backward to forward was confirmed experimentally, i.e. in the case of an internal type for the stator-limiter in the direction of rotor rotation. Identification of dynamic behavior is made on the basis of eigenfrequencies and eigenmodes, motion orbits of an eccentric point (on the rotor), Campbell diagrams and AFC. The calculation of such characteristics has done using an original mathematical approach developed by the author earlier in order to describe the backward motion of common rotor on an external stator. A good agreement is obtained between the theoretical frequencies and amplitudes of vibration and the experimental ones. Therefore, the author's technique is also suitable for the revealed forward rotor motion around the internal stator.

Keywords: shaft, contact, continuous/inseparable interaction, supersynchronous motion.

Nomenclature

$\boldsymbol{E}$	Identity matrix
$[K]$	Stiffness matrix of contactless system (without the contact and with the infinite clearance between rotor and stator)
$[\tilde{K}]$	Stiffness matrix of contact system (with the contact and zero clearance between rotor and stator)
$[M]$	Inertia matrix of rotor-stator contactless system
$\{A\}_i$	Real amplitudes for physical displacements of rotor/stator before their contact in a band of the ith dominant frequency of natural oscillations of the contactless system
$\{\tilde{A}\}_i$	Real amplitudes for physical displacements of rotor/stator after their contact in a band of the ith dominant frequency of natural oscillations of the contact system
$\{u\}_i$	Modal displacements for the ith eigenfrequency of contactless system
$\{\tilde{u}\}_i$	Modal displacements for the ith eigenfrequency of contact system
a_i	Modal amplitude for the ith eigenmode of contactless system with the finite clearance and touching between rotor and stator, i.e. Without pressure/support of rotor on stator and a_i is equal to the ratio of δ to $u_{2k-1\ i}$
$u_{2k-1\ i}$	The k-th modal displacement in the contact section in the ith eigenmode of contactless system
δ	Radial clearance in the contact section
η	Coefficient of hysteresis losses in the system materials
λ_i	The ith eigenfrequency of contactless system
$\tilde{\lambda}_i$	The ith eigenfrequency of contact system
μ	Friction coefficient of slipping
$\omega(f)$	Rotary velocity (frequency) of rotor
$\omega R/\delta$	Whirl velocity of rotor at the forward clear rolling on stator
$\Omega(\Omega)$	Whip velocity (frequency) of rotor at the forward rolling with whipping and slipping on stator

1. Introduction

In some rotating machinery, such as centrifuges, washing machines, and superflywheels (gyroscopic energy storage), the relatively rigid rotor is supported by very compliant bearings. The supercritical work and using complexity of the viscous dampers enforce to introduce into a design amplitude limiters of rotor oscillations, i.e. its whirling or/and whipping. The limiter works only in emergency situations, when the whirl/whip amplitude exceeds the specified clearance between rotor and limiter, i.e. the stator. The slipping of rotor on the stator in the specified position prevents the friction between rotor and stator in other places. Stiffness of the limiter is usually much greater than that of bearings. Sometimes with that, it is an internal cylinder inside the hollow end of rotor (Fig. 1).

Despite of the design simplicity there are no results of mathematical and natural modeling for the outer rotor – inner stator system and its unseparated dynamics. And this is despite the rather extensive and fresh scientific and technical literature on a similar problem for a typical rotor system with outside stator [1-10].

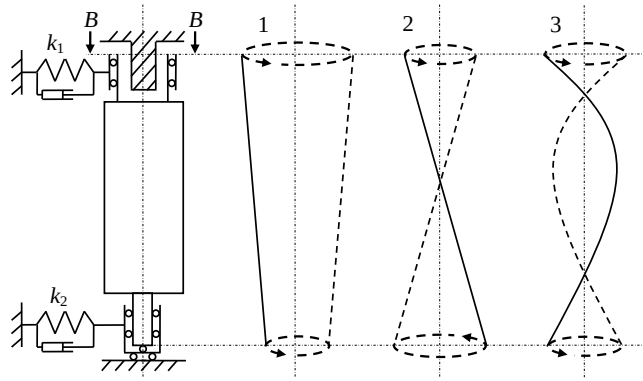

Fig. 1. Scheme of rigid rotor on elastic bearings with stator inside

2. Outer rotor – inner stator model

The rotor is assumed to be rigid and axisymmetric, and also supported on unequal linear elastic bearings (Fig. 1). Also shown are two characteristic modes of natural oscillations of the rotor under such conditions: 1 – cylindrical and 2 – conical. An uncharacteristic third mode is high-frequency rotation at speeds when elastic deformation of the rotor itself occurs, i.e. in the vicinity of the first natural or bending frequency of the rotor on rigid bearings.

In some cross sections, the transverse whirl displacements of a rigid rotor on elastic bearings differ little from the whipping of a flexible rotor on rigid bearings. This fact allows transferring the results from one rotary model to another. Fig. 2 shows a comparison of a rotor previously researched under various conditions of its rolling without and with whipping and slipping along an external stator-limiter [10], as well as a rotor recently experimentally examined with an internal-type stator-limiter.

Modification to the previously materialized setup was minimal. It is reduced to a nozzle of cap on the end of cantilevered steel shaft 645 mm long and 8 mm in diameter. The cap is a hollow aluminum cylinder with an inner working diameter of 12 mm, an LED, a 3 V coin cell battery and a total weight of ≈ 20 g. As well as it is replaced the end support with a clearance (which had a sleeve with an inner diameter more than 8 mm) on a support made of steel and plexiglass of suitable size, in which a rod with a diameter of 10 mm made fluoroplast-4 or steel and was rigidly fixed (inside its sleeve made of plexiglass).

Look at the schemes of contact loading and non-separated motion of the discussed systems (Fig. 3), we can conclude that the B–B type of interaction is preferable to the A–A type. In a B–B

type system, the resulting F_c from the normal contact force N and the dry friction force μN causes the rotor whirling in the direction of rotation, which helps to reduce internal stresses (in the rotor). However, the above obvious was not confirmed by experiments due to the positive supersynchronous velocity of whirl/whip ($\Omega > \omega$).

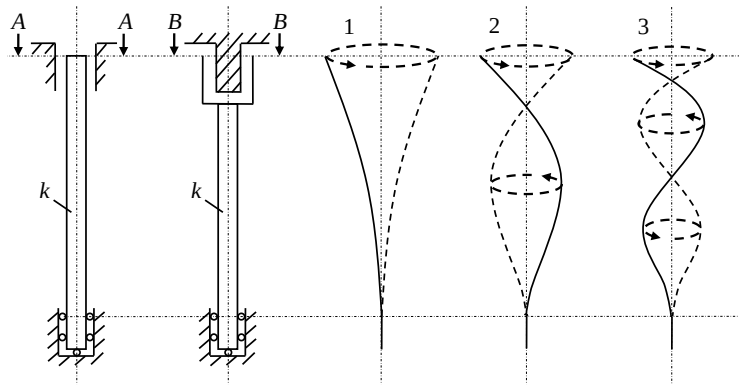

Fig. 2. Scheme of experimental flexible rotor on rigid bearings with stator outside [10] and inside

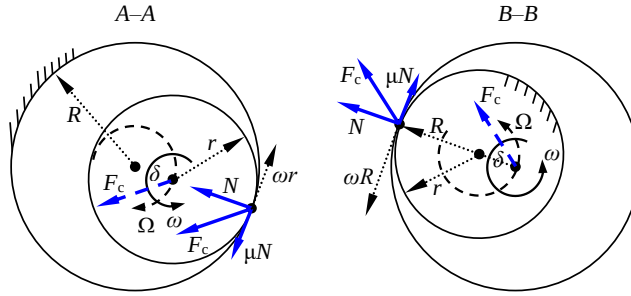

Fig. 3. Contact forces and whirling directions of rotor rolling with its outer and inner surface around stator

3. Summary on dynamics

In general, transformation of the previously tested flexible rotor into a hollow, point-like light on it, transparency of the constructed internal support and photography with long exposure made it possible to observe the real trajectories of eccentric Fig. 4, the effect of clearance geometry, directions, ranges Table 1, velocities Fig. 5(a) and amplitude Fig. 5(b) of the rotor whirl/whip at rolling around the stator with its inner surface. Author's photos (Fig. 4) and all other related results are received recently in Vibromechanics Laboratory of the Mechanical Engineering Research Institute.

In particular, the orbits have always been with loops facing inwards (towards the rotor axis). The directions of trajectories were always forward, i.e. in the direction of rotation of rotor. The ratio r/δ, where $\delta = R - r$ is the radial clearance between contact surfaces, R is the radius of outer (r – inner) contact surface, sets a maximum number of loops, i.e. in case of rolling without whipping and slipping. The fraction R/δ is equal to a maximum number of forward whirling (i.e. revolutions of the axis) of the rotor in one revolution of its own rotation, and multiplying R/δ by the rotation speed ω gives the angular velocity of clean rolling.

In an usual system with rotor inside and stator outside, during the rolling and whip phenomenon: the trajectory loops are turned to a periphery (from the rotor axis), the ratios R/δ and r/δ set the largest number of loops and backward whirling respectively for each rotation of the rotor, the product $\omega r/\delta$ is equal to velocity of the rolling without whipping and slipping.

Table 1. The effect of clearance geometry, directions, ranges

Vertical, steel, round ($r = 4$ mm) shaft with hollow cylinder (at the end)								
	No. startup-shutdown	Ratio $\frac{R}{\delta}$	Materials		Highest frequency of rotation f_{max}, Hz	Ranges R_i of rotation frequencies in case of stable rolling with slipping, highest frequencies Ω_i and amplitudes A_{max} of forward whirl/whip in corresponding speed ranges		
			Shaft at the point of contact - stator rod	Friction coefficient of slipping (μ)		R_i, Hz	Ω_i, Hz	A_{max}, mm
Contact characteristics of the system in series of "rolling" tests	1	6	Aluminum – fluoroplast-4	0.11	96	5-49	51	0.31
						66-96	54	0.3
	2	6	Aluminum – steel	0.2	88	5-48	62	0.22
						71-88	66	0.22
	3	6	Aluminum – steel	0.2	76	6-48	68	0.21
						48-52	186	0.27
						61-76	341	0.29
						50-22	98[I]	0.1
	4	6	Aluminum – steel	0.2	76	5-60	69	0.29
						60-76	180	0.39
	5	5.5	Aluminum – steel	0.2	83	4-50	68	0.23
						50-52	278	0.26
	6	5	Aluminum – fluoroplast-4	0.14	92	5-46	51	0.31
						75-92	66	0.3
						54-50	159	0.35
						50-44	57	0.34
						44-5	68	0.3
	7	4.33÷3	Aluminum – steel	0.2	79	5-59	69	0.3
						30-71	93[I]	0.17
Dynamic characteristics (averaged) of the system	Lowest natural frequencies of non-rotating shaft after series of tests (Hz)					Loss factor inside the rotating shaft after series of tests (η)		
	As unsupported on stator		As supported on stator					
	10, 74, 212, 420		60, 191, 390			0.003		

The appearance of supersynchronous velocities or frequencies $\Omega_i > R_i$ is taken as the main attribute of rolling with whipping and slipping (Table 1). For example in experiment No. 1, supersynchronous oscillations was recorded in a shutdown phase at the rotation frequencies from about 40 to 10 Hz (Fig. 5). An additional attribute of rolling with whipping and slipping was the occurrence of specific trajectories for the rotor eccentric point with inward-looking loops (Fig. 4). Subsynchronous frequencies $\Omega_i > R_i$ are also indicated in table 1 as accompanying the rolling with whipping and slipping, because their values differ little from those detected during supersynchronous motion, and they are characterized by orbits with one or more loops facing the rotor axis for any of its eccentrics and simultaneously circular whirling of the rotor axis itself. For example, subsynchronous rolling with whipping and slipping was observed during shutdown No. 1 and rotation frequencies from about 100 to 65 Hz (Fig. 5), while when synchronous motion occurred in the range of ≈ 65-40 Hz, the all rotor orbits (of axis and eccentrics) were circular.

Theoretical parameters for the i-th form of rolling with whipping and slipping in the Fig. 5 are determined by the author's method [10]. The discussed systems (Fig. 1, 2) are simulated mathematically and enough lightly in the finite element formulation:

$$[M]\{\ddot{q}\} + (1 + i\eta)[K]\{q\} = -e^{i\psi}\{f_N\}, \quad (1)$$

where $\{q\}$ are complex displacements of rotor sections with concentrated mass and transverse inertia moment, $\{f_N\}$ is vector of contact forces dominating over all other system forces, i.e. for

instance $\{f_N\} = N(1 + i\mu)\,\{0,\ldots,0,1,0,\ldots,0\}^T$ as general case where 1 corresponds lateral displacement of contact section or kth section with the δ-clearance between rotor and stator, ψ is whirl angle of contact forces or rotor axis in the contact section, η is positive value at the forward whirl and negative value at the backward whirl. Let it is the original system, consisting of a rotor on two or n bearings.

Fig. 4. Orbit evolution of the eccentric during continuous forward whirling with whipping and slipping of the "outer" rotor on the "inner" stator with an increase of rotary velocity as rev/min (Startup No. 5, September 2022)

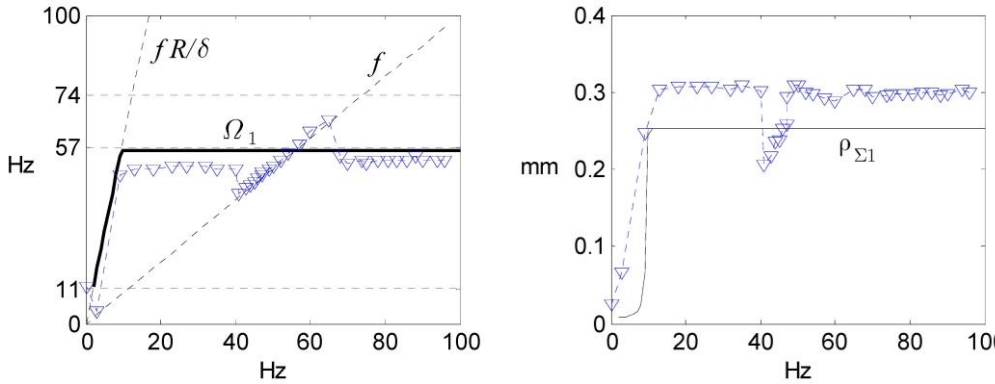

Fig. 5. Measured at startup No. 1 (▽) and theoretical frequencies and amplitudes of the whirling for the steel experimental rotor rolling without and with whipping and slipping around the "internal" stator, i.e. a) Campbell diagram of the rotor and b) its amplitude characteristic by rotary frequency

On the other hand, an equivalent system with rotor on the $n + 1$ supports and zero clearance in the contact section can be considered, governed by the matrix equation, which at the same time is locally destabilized by the opposite forces $N(1 + i\mu)$:

$$[M]\{\ddot{\tilde{q}}\} + (1 + i\eta)[\tilde{K}]\{\tilde{q}\} = e^{i\psi}\{f_N\}, \tag{2}$$

wherein the matrix $[\tilde{K}]$ differs from $[K]$ only by an adding of relevant contact stiffness k_k between kth rotor section and stator.

Obviously, solutions of the written equations can be assumed in the harmonic forms:

$$\{q\} = e^{\pm i\Omega t}\{A\}, \quad \{\tilde{q}\} = e^{i(\pm\Omega t+\gamma)}\{\tilde{A}\}, \quad \{\rho_\Sigma\} \approx \{A\} + \{\tilde{A}\}, \tag{3}$$

where γ is lag for the whirl/whip displacements of equivalent system relative to the original one by an amount equal to the friction angle, i.e. satisfying the identity $\mu = \tan\gamma$.

So, it can be derived a fundamental equation of rolling which includes square of velocity Ω and doesn't depend from sign of Ω:

$$(\Omega^2[M]-[K])\{A\}_i=\left(\left[\widetilde{K}\right]-\Omega^2[M]\right)\{\tilde{A}\}_i, \tag{4}$$

or

$$\boldsymbol{E}\{\tilde{A}\}_i=\left(\left[\widetilde{K}\right]-\Omega^2[M]\right)^{-1}(\Omega^2[M]-[K])\{u\}_i a_i. \tag{5}$$

As a result, the used method yields that frequencies and amplitudes of vibration in case of the rolling with whipping and slipping are defined by dominating natural frequencies and modes of the rotor:

$$\begin{gathered}\Omega_i\approx\tilde{\lambda}_i\left(1-\frac{1}{2}\frac{\eta/\mu}{1+\eta/\mu}\right),\\ \{\tilde{\rho}_\Sigma\}_i\approx\{A\}_i+\{\tilde{A}\}_i=\{u\}_i\frac{\delta}{u_{2k-1\ i}}+\frac{\Omega_i^2-\lambda_i^2}{\tilde{\lambda}_i^2-\Omega_i^2}\{\tilde{u}\}_i\{\tilde{u}\}_i^T\{u\}_i\frac{\delta}{u_{2k-1\ i}}.\end{gathered} \tag{6}$$

4. Conclusions

For the first time, the real motion of rotor is demonstrated, which accompanies the rolling phenomenon of an outer rotor on an inner stator.

The universal calculation method is proposed for all rotary contact systems that predicts a frequency and amplitudes of the whirling and whipping associated with rolling and slipping of rotor on stator.

Acknowledgements

The authors have not disclosed any funding.

Data availability

The datasets generated during and/or analyzed during the current study are available from the corresponding author on reasonable request.

Conflict of interest

The authors declare that they have no conflict of interest.

References

[1] N. Salvat, A. Batailly, and M. Legrand, "Two-dimensional modeling of unilateral contact-induced shaft precessional motions in bladed-disk/casing systems," *International Journal of Non-Linear Mechanics*, Vol. 78, pp. 90–104, Jan. 2016, https://doi.org/10.1016/j.ijnonlinmec.2015.10.001

[2] N. Vlajic, A. R. Champneys, and B. Balachandran, "Nonlinear dynamics of a Jeffcott rotor with torsional deformations and rotor-stator contact," *International Journal of Non-Linear Mechanics*, Vol. 92, pp. 102–110, Jun. 2017, https://doi.org/10.1016/j.ijnonlinmec.2017.02.002

[3] T. Popp, H. Stibbe, D. Heinisch, H. Reckmann, and P. Spanos, "Backward whirl testing and modeling with realistic borehole contacts for enhanced drilling tool reliability," in *IADC/SPE Drilling Conference and Exhibition*, Mar. 2018, https://doi.org/10.2118/189600-ms

[4] J. C. Wilkes, "Application of Dry-friction whip and whirl solution methods to systems with support asymmetry," in *ASME Turbo Expo 2018: Turbomachinery Technical Conference and Exposition*, Jun. 2018, https://doi.org/10.1115/gt2018-76991

[5] U. Ehehalt, O. Alber, R. Markert, and G. Wegener, "Experimental observations on rotor-to-stator contact," *Journal of Sound and Vibration*, Vol. 446, pp. 453–467, Apr. 2019, https://doi.org/10.1016/j.jsv.2019.01.008

[6] E. G. Ovy, "Suppression of rubbing in rotating machines by lemon-type bearing," *Journal of Vibration and Acoustics*, Vol. 141, No. 5, Oct. 2019, https://doi.org/10.1115/1.4043817

[7] M. Behzad and M. Alvandi, "Friction-induced backward rub of rotors in non-annular clearances: Experimental observations and numerical analysis," *Tribology International*, Vol. 152, p. 106430, Dec. 2020, https://doi.org/10.1016/j.triboint.2020.106430

[8] Y. Briend et al., "Dry-whip phenomenon in on-board rotordynamics: Modeling and experimentation," *Journal of Sound and Vibration*, Vol. 513, p. 116398, Nov. 2021, https://doi.org/10.1016/j.jsv.2021.116398

[9] A. K. Srivastava, M. Tiwari, and A. Singh, "Identification of rotor-stator rub and dependence of dry whip boundary on rotor parameters," *Mechanical Systems and Signal Processing*, Vol. 159, p. 107845, Oct. 2021, https://doi.org/10.1016/j.ymssp.2021.107845

[10] A. N. Nikiforov, *Applied Semi-Empirical Theory for Non-Separated Motion of Rotor on Stator*. (in Russian), Saint-Petersburg: SUPER Publishing House, 2021, https://elibrary.ru/ktaeka

Andrey Nikiforov is working as a research associate at Mechanical Engineering Research Institute of the Russian Academy of Sciences. His main research areas are contact dynamics of rotor-stator systems, waves and oscillations for rotor partially filled with fluid.